Improved Modified Embedded Atom Method Potential for SiGe

Xiaohan Zhang, Yanming Wang, Livia B. Pártay, Wei Cai

[a]*Department of Mechanical Engineering, Stanford University, California, 94305-4040*

Abstract

Outline: Key message: The discrepancy of critical dislocation nucleation strain between atomistic predictions and experiments is significantly reduced by a new interatomic potential. The potential demonstrates several advantanges over the widely used SW and Tersoff potentials, predicting more accurate thermal and mechanical properties relevant to dislocation nucleation. Introduction: SiGe/Si epitaxy system is important Dislocation nucleation in SiGe/Si critically limits the yield of modern chips. (maybe rephrase SGC nucleation paper for this part) A wide discrepancy between the numerical prediciton and experiments exists. Experimental nucleation strain is much less than atomistic predicitons. cite Maras 2016, 2017, Nix, etc. One of the primary factors contribute to the discrepancy is potential artifact, other factors include the dominant dislocation mechanism. surface conditions. potential artifact. A review of thermal and mechanical properties of SW and Tersoff indicates potential problems related to dislocation nucleation in SiGe. SW(Ge) melting temperature is off by twice, suggesting bonds are strong leading to overestimation of critical strain. Tm is related to bond strength. (need argument). Tersoff model is too stiff to predict ductile brittle transistion behaviors (evidence needs to be searched). Motivation of this work. This work shows that a more accurate atomic potential is capable of reducing the discrepancy from ??% to ??%. The potential predicts accurate LC, Cxx, Tm, Em, Es, etc, all relevant to dislocation nucleation process. Is NEB and MD consistent? Organization of the paper: (sec 2) Method + LC. (sec 3) NEB+MD result. (sec 4) Tm + Cxx (+ Em + Es). Method (potential development): An MEAM potential is developed based on the state-of-art functional form and fit it to experimental values of zinc-blende bulk modulus, lattice constant and cohesive energy. The functional form is derived based on CPL2008. Some problems identified in reproducing results of CPL2008. How this potential is related and improved based on CPL 2008. Lattice constant match closely with experiments. (PLOT1. lattice constants vs experiment) NEB+MD: (PLOT2. cell of bulk shearing and surface pit.) 1) Stress strain curve at finite temperature shows that MEAM has softer bonds leading to earlier critical strain. (PLOT3. ss curve on top of SW). The motivation and effectiveness of surface pit. cite SGC paper. MEAM leads to lower energy barrier for the same xGe. (PLOT4. Eb vs strain, MEAM on top of SW) 3) MD shows shuffle-glide dislocation complex. A new evidence to the mechanism which is used to be considered as an SW artifact. cite Godet04, SGC paper. Tm+Cxx+Em+Es: The dislocation nucleation is a complicated process involving several mechanisms. An impirical interatomic potential usually cannot address many properties

*Corresponding author. E-mail address: caiwei@stanford.edu (Wei Cai).

correctly at the same time. Here we show some essential properties that are relevant to dislocation nucleation can be sufficiently captured by the potential. Elastic properties: (SIPLOT1 C11, C44. on top of Tersoff) *** Why Elastic properties are relevant? (Mention in text, but results shown in appendix) 1) bulk modulus is the most straight forward mechanical properties that can be accurately calibrated (cite?). For epitaxy system, modulus is compromised by the presence of free surface. However, an effective potential must be able to predict accurate modulus in order to be applied to epitaxy system modeling. *** Why Tm is relevant to dislocation nucleation? 1) Modern deposition technique such as CVD, unlike traditional molecular beam epitaxy, requires higher temperature operating environment so that the atoms stay near equilibriua and do not form islands during the deposition process. The increased temperature is above 800K which gets close to the melting point of semiconductors. If the potential has wrong prediction of Tm, the simulation at this high temperature is not trustable (why?) 2) Melting point is an indicator of the strength of bonds (why?). Dislocation nucleation process is essentially breaking of bonds due to excessive local stress. Therefore, the incepient process of the nucleus critically depends on the bond strength. If the bond is overstiff, the critical strain will be inevitably overestimated. (why?) *** How Tm is calculated? 1) Tm is first approximated with NS calculations. (Any new developments and understanding about NS calculations of SiGe ?) 2) The phase diagram of SiGe involves a wide solidus and liquidus temperature difference, which we shall address more carefully in subsequent works. Here we use two-phase coexistance method to give an error bar on the Tm curve. Melting temperature: (PLOT5. Tm vs xGe, on top of SW that connects Si and Ge). SI. NS calculation details. (SIPLOT2 Cvp vs T plot). 3) The result shows that the potential sufficiently agrees with experiments, with an error bar of (??)K. Migration energy barrier. (PLOT6. Eb vs xGe. on top of exp (scattered points)). *** Why migration energy barrier is relevant? point diffusion is the most relevant mechanism forming frank-partial loop in CVD. cite() Surface energy. (Mention in text) *** Why surface energy is relevant? surface nucleation of dislocation is the most commonly observed nucleation mechanism. bond breaking on the free surface is closely related to surface energy (why)

Keywords:
dislocation nucleation, semiconductor, SiGe Meam, Energy Barrier Calcualtion, Nested Sampling

1. Introduction

As semiconductor devices dimensions become smaller, built-in internal stress becomes an indispensable strategy to reach the target electronic performance. Under such high stress and confined geometries, controlling the nucleation, migration, and multiplication of dislocation defects becomes extremely important. The nucleation of dislocations not only reliefs the strain (thus degrading the electronic performance) but also can damage the device by providing a short circuit if they multiply and migrate away from their nucleation site. On the other hand, certain types of dislocations are beneficial if they are formed in a controlled manner, such as in the stress memory technology (SMT).

Dislocation nucleation during the deposition process of a semiconductor device happens on the time scale

of a few nanoseconds [cite Rabier] [cite annealing nucleation] thus the problem can be sometimes studied by brute-force MD simulations [cite Godet, Pizagalli], which allows capturing dislocation nucleation events by simulating more realistic sized systems than ab-inito calculations. Nudged Elastic Band or string methods are also informative technologies for they can quantify the nucleation energy barrier at 0K, which combined with the prefactors (obtained with a large number of finite temperature MD simulations) gives the statistical nucleation rate. However, to make faithful predictions, all the atomistic methods require efficient but faithful interatomic potentials in terms of both mechanical and thermal behaviors. Specifically, the environment for semiconductor fabrication is characterized as high stress and high temperature. The intentionally introduced stress can reach to 3 GPa, and the temperature varies from 800K to 1000K [this is Samsung condition. need to find literature]. As will be shown by the brief survey below, SW and Tersoff, two widely used potentials for silicon and germanium, are not suitable for the studies under those conditions.

Previous numerical studies with SW potential [cite SW1985, 1992] exhibit correct behavior for modeling shear properties and nucleation in silicon nanowires when compared to *ab-initio* calculations (Godet et al. (2009) Pizzagalli et al. (2013)). SW has been also extensively used for dislocation nucleation in silicon for its success in predicting various mechanical and thermal properties of silicon. However, it has been shown that SW cannot accurately predict the melting temperature of Ge Ryu and Cai (2008), overestimated by twice as high as the experimental measurement. As will be shown in Section **??**, the melting temperatures of different compositions for $Si_{1-x}Ge_x$ are likewise seriously overestimated. This deficiency of SW makes its prediction at high temperature, especially at the $900 - 1100$K regime, not faithful. On the opposite side, Tersoff potential is preferred when modelling high temperature solid state behaviors such as amorphous core shell nanowires [cite Shan] but leads to over-stiffer stress-strain response than that from experiments [cite]. It thus appears that a potential that has a good mechanical properties at high temperature is indispensable. This work improves an existing MEAM potential based on the state-of-art functional forms and demonstrate its qualification for our purpose.

MEAM has demonstrated correct behaviors for the brittle-to-ductile transition of silicon, for example in Kang and Cai (2007, 2010)). Kang and Cai (2007) also presents a systematic performance comparison between SW and MEAM with respect to brittle-ductile transition behavior of silicon. Minor changes have been proposed along the way of developing MEAM. These include changes in the form of the angularly dependent electron density term to make them orthogonal,[11], different ways to sum the partial electron density terms[12] and changes to the original screening functions to remove discontinuity[13]. There have been similar attempts for embedded atom method (EAM), which has been applied by Glue Model [3], Finnis-Sinclair [4] or Volter-Chen [5] type CPL 2010 to model material properties over a large range of phase space.

YANMING: can you rewrite this paragraph. For now, I state that our potential is built upon CPL2010 and explain why. We need to highlight what went wrong with CPL 2010 and what we have improved. Our work builds on the latest MEAM potential reported by Grochola et al. (2010) who uses the new and improved

electron density summing functions as well as the improved screening functions for silicon and germanium. It also includes a correction to the Si potential to fix an anonymous liquid radial distribution function. The potential functional form is consistent with Baskes (1992), where angularly dependent metallic forces are introduced to allow more accurate description of FCC (Lee et al. (2003)), BCC(Lee et al. (2001)) and HC(Kim et al. (2006)). Similar alloy SiGe MEAM potentials have been proposed and applied by Swadener and Picraux (2009) andRead and Tewary (2007) however their potentials contain the earlier problematic screening functions. this statement from CPL2010 needs to be verified

We applied two specialized methods to demonstrate the qualification of the improved MEAM potential. We use a modified string method to quantify the energy barrier for a shuffle dislocation to nucleate from a thin film, the free surface of which is disturbed by a rectangular surface pit. The modified string method is developed based on NEB method, but provides better numerical stability. The Nested Sampling method is used for estimating the melting temperature of the SW and MEAM potentials for a few compositions. Livia: can you put in a short description of NS method here. Nested Sampling is a recently developed free energy sampling method which does not require a priori knowledge of the alloy structure.

The paper is organized as following. Section 3 describes the fitting procedure used for fitting the SiGe alloy systems and the corrective terms. The resulted parameters are tabulated in Table 1. Energy barrier and melting temperature calculations are presented in section 4 and 5.1.1 separately. Some conclusions are drawn in the end.

2. Tech details to be commented out

Notes on SiGe meam potential:

1. Dr. Mike Baskes suggests us to borrow the new (CPL 2010) SiGe potential (instead of the original PRB 1989 SiGe potential). A modified embedded atom method interatomic potential for alloy SiGe Chemical Physics Letters Gregory Grochola *, Salvy P. Russo, Ian K. Snook.
2. potential file: library.meam. cross potential file: SiGe.meam
3. element,

   use Ge or Ge5. Ge and Ge5 are only different for the last 2nd parameter which is a scaling parameter that only takes effect for the binary system.

   use Si4 or Sijpcm. Si4==Sijpcm. Siz is different only for the last 2nd parameter as well.

4. Problem found for the previous cross potential file:

   In AuSi2nn.meam, (1,1) => gold. (2,2) =>silicon.

   Should copy (2,2) params to SiGe.meam.

   The correct numbers to put in SiGe.meam should be:

   attrac(1,1)=-0.36

repuls(1,1) = 16

Cmin(1,1,1) = 1.85

rc = 4.5

note: Cmin(1,1,2), (2,1,1)(2,2,2) from CPL 2010 paper. Cmax = 2.8 as default.

delta(1,2) = cohesive energy difference

alpha(1,2) = $(9B\Omega/Ec)^0.5(Eq.4)$

one should not change delta and alpha

5. Improvements on the lattice calculation in CPL 2010 paper:

   1) fix typo, lattice const is not re.

   2) no correction term to Si (erose?)

   3) Si and Ge lattice constants do not match experiments. The fitting approach is not clear.

6. **How to enable erose_form=3 in Lammps**

   A) Do "diff" between MD++/meam and lammps/meam folder, the only difference is the meam_setup_done.F: B) Download and install lammps-11Aug17/ C) Put the lines between 944 to 953 of meam_setup_done.F from MD++ and paste them to the same position of lammps-11Aug17/lib/meam/meam_setup_done.F 3) recompile meam 4) In SiGe.meam, add erose_form = 3 in the bottom.

7. **Test case to use erose_form = 3 with AuSi.meam**

   Follow wiki page and the above instructions, potential evaluated of the FIRST step should be consistent with EPOT.txt. This is verified.

3. Methods

3.1. Fitting procedures for SiGe alloy Yanming, please review this section.

We follow Baskes' Modified Embedded Atom Method approach. We refer the readers to Baskes (1992) for full details of MEAM. For a description of the second nearest neighbour methodology see Lee et al. (2003). For a description of the screening function used in this work see Baskes (1997). For a description of how to construct alloy potentials in the MEAM formalism see Lee et al. (2001).

The MEAM model describes the potential energy of an atomistic system with atoms located at $\mathbf{r_i}$, $i = 1, ..., N$ by the following equation:

$$V(\{\mathbf{r}_i\}) = \sum_{i=1}^{N} F(\bar{\rho}_i) + \sum_{i=1}^{N-1} \sum_{j=i+1}^{N} S_{ij}\phi_{ij}(|\mathbf{r}_i - \mathbf{r}_j|) \tag{1}$$

The three fitting targets include the bulk modulus, lattice constant and the cohesive energy. The cohesive energy of the fitted $Si_{0.5}Ge_{0.5}$ zinc-blende crystal structure can be written as

$$E_{ij}^{ZB}(R) = 1/2\left[F_i(\bar{\rho}_i) + F_j(\bar{\rho}_j) + Z^{ij}\phi_{ij}(R)\right] \tag{2}$$

where $F_i(\bar{\rho}_i)$ and $F_j(\bar{\rho}_j)$ are the embedding energies of alloy atoms i and j. $\phi_{ij}(R)$ is the cross interaction and Z^{ij} are the number of first nearest neighbours.

The cross interaction potential takes the form of

$$\phi_{ij}(R) = E_{ij}^{ZB}(R) - 1/2\left[F_i(\bar{\rho}_i) + F_i(\bar{\rho}_i)\right] \tag{3}$$

The value of the energy per atom for the equilibrium reference structure is obtained from the zero-temperature universal equation of state by Rose et al. (1984) as a function of nearest-neighbor distance R as follows,

$$E^u(R) = -E_c(1 + a^* + da^{*3})e^{-a^*}, \tag{4}$$

where d is an adjustable parameter, and $a^* = \alpha(R/r_e - 1), \alpha = (9B\Omega/E_c)^{1/2}$.

The equilibrium lattice constant of $Si_{1-x}Ge_x$ can be approximated by the a function of the compositions of germanium element as,

$$a(x) = (5.431 + 0.20x + 0.027x^2)\text{Å, at } 300K$$

For the potential to fit with lattice constants, we create a large Si crystal and randomly replace Si atoms with Ge atoms. The simulation is performed with free box. Then the volume is computed to predict the lattice constants at equilibrium. We managed to get the values of the lattice constants for different Ge compositions at both 0K and 300K.

Details to be removed or go to appendix: For the current fitting, we do not include the 2nn correction made by Seunghwa on Si Ryu et al. (2009). This can be added by further modifying the SiGe.meam file. We constructed a library.meam file that contains one entry for Ge MEAM potential, with the name as Ge5. It is the file that is used for Au-Ge potential development.

With the parameters presented in table .1, the lattice constants fit to the experiments Dismukes et al. (1964). The fitting process is different from Grochola et al. (2010) in the sense that the parameter for pure Si is adopted from Ryu et al. (2009), and also that the cross potential is modified to make the lattice constant right.

Table 1: IMEAM model parameters for Si, Ge, and SiGe alloy potential (currently from Grochola 2010)

Element	E_c	r_e	R_{cut}	B	A	$\beta^{(0)}$	$\beta^{(1)}$	$\beta^{(2)}$	$\beta^{(3)}$	$t^{(1)}$	$t^{(2)}$	$t^{(3)}$	$C_{\max}$	$C_{\min}$	d
Si	3.85	2.45	4.5	0.77	0.66	3.95	2.0	0.0	7.5	2.9	5.77	-2.2	2.8	1.41	0.0
Ge	4.63	2.35	4.5	0.99	0.58	3.55	2.5	0.0	7.5	1.8	5.25	-2.61	2.8	1.41	0.0
SiGe	4.23	5.529	4.5	0.88									2.8	1.41	0.0

We managed to put MEAM parameters of paper Grochola et al. (2010) into lammps to reproduce their results for lattice constants. The elastic constants for SiGe can be extracted from the simulations: C11 = 181.03 GPa, C12 = 80.57 GPa, and C44 = 85.36 GPa, which quantitatively agree with experimental measured values. In the meanwhile, we found several critical issues to use the potential of Grochola et al. (2010). I1) the correction functions to modify the radial distribution function of the liquid alloy developed

in the paper is not implemented in LAMMPS. Although, it should not have significant effects on simulations of solid devices. I2) a mistake is identified in the parameter table for the r_e column. I3) The claimed experimental lattice constant to fit is 5.5285Å, but the actual experimental value is 5.5377Å. I4) How the lattice constant curve is obtained was not clearly stated. However, from the results, one can infer that the data should be obtained from finite temperature simulations, because otherwise the lattice constant of Si is not 5.431Å. Then curves are shifted to match the lattice constant of Si with experimental value.

We reproduce the potential of Grochola et al. (2010) as shown in Fig. 1, which demonstrates that their potential deviates from the experimental results, especially for composition of Ge near 0.5 the potential underestimates the lattice constant.

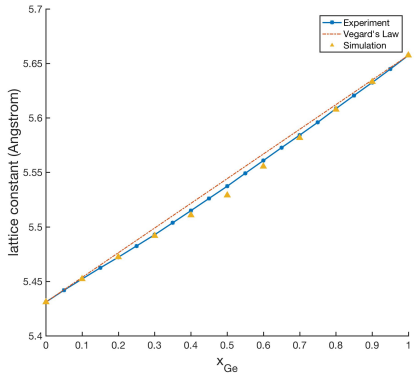

Figure 1: Lattice constants of $Si_{1-x}Ge_x$.

The parameters of the SiGe MEAM potential are determined as follows. The MEAM parameters for pure Si and Ge are adopted from our previous work Wang et al. (2016); Ryu et al. (2009), where a revised EOS function is proposed to correct the melting point prediction particularly for Si. The set of parameters for the Si-Ge cross interactions is given by Table 2. In Table 2, Si and Ge are labeled as Element 1 and 2 respectively. The parameters of $E_c(1,2)$, $\Delta(1,2)$, $\alpha(1,2)$ and $r_e(1,2)$ are chosen to reproduce the cohesive energy, lattice constant and bulk modulus of $Si_{0.5}Ge_{0.5}$ with an orderly zinc-blende structure, predicted by DFT calculations Grochola et al. (2010). The relative electron density of Si $\rho_0(1)$ is tuned, in order to fit the relation between the lattice constant and Ge fraction to experimental observations for Si-Ge solid solution. As shown in Fig. 2, the lattice constants predicted by MEAM are in very good agreement with the experimental data. Comparing with the estimation by the Vegard's law, a linear combination of the lattice constants of the two species, the MEAM does a distinguishably better job. Finally, the screening parameters $C_{\max}$ and $C_{\min}$ for the cross potential are directly adopted from the existing Si-Ge MEAM potential Grochola et al. (2010), but these parameters are adjustable, which can potentially provide extra degrees of freedom for fitting to other material properties Wang et al. (2016); Ryu et al. (2009).

Table 2: Parameters for SiGe cross potential

$E_c(1,2)$	$\Delta(1,2)$	$\alpha(1,2)$	$r_e(1,2)$	$\rho_0(1)$	r_c	$C_{\max}$	$C_{\min}$
4.23	0.01	4.9716	2.3939	1.2719	4.5	2.80	1.41

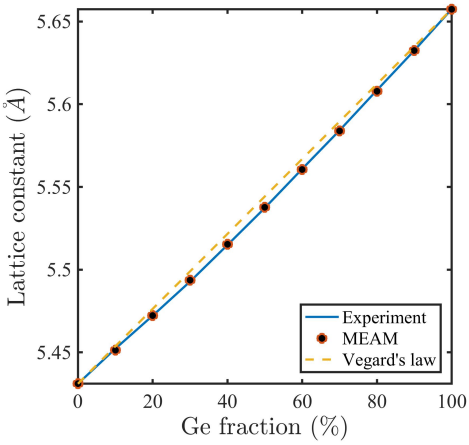

Figure 2: Lattice constants of $Si_{1-x}Ge_x$.

3.2. Molecular Dynamics

We use Lammps (Plimpton (1995)) for all finite temperature Molecular Dynamics simulations. Verlet algorithm for time integration is adopted for time steps of 0.5fs. We applied Nosé-Hoover thermostat in NVT ensemble to maintain the system at desired temperature levels, from 400K to 1400K. The bulk simulation for the stress-strain curves include 14400 atoms. The simulation cell of the thin film has a dimension of 192Å(x), 192Å(y) and 214Å(z) and contains 3.6×10^5 atoms. The free surface of the thin film is created by expanding the simulation box 1.2 longer in the z direction. Periodic boundary conditions are applied to both x and y directions. A surface pit is created on the (001) surface with a depth of 21.4Å. A compressive strain is applied along [110] direction, at the strain rate of $2 \times 10^8\, s^{-1}$.

3.3. Nudged Elastic Band method

A modified NEB method is applied to find saddle points and the associated Minimum Energy Path (MEP). The method takes a chain of atomic configurations as input and performs constrained relaxation on each node until it finds the MEP while maintaining equal spacing to neighboring images. Thus, every configuration is allowed to relax independently. This is different from the traditional NEB or string method where constraints are applied during the relaxation. After a predetermined number of relaxation steps, the path is reparametrized between the two endpoints using linear interpolation between each of the existing configurations. The location of these new interpolated configurations is such that the path is equally divided

with a constant distance (in phase space) between each neighboring pair of configurations. This new algorithm runs efficiently in parallel mode and overcomes several difficulties occurred in classical string methods such as instability and poor discretization when applied to high-stress conditions and/or to semiconductors.

The simulation cell for all NEB calculations has a size of 81.4Å(x), 81.4Å(y) and 114Å(z), containing 14400 atoms. The free surface of the thin film is created by expanding the simulation box by 20% in the z direction. Periodic boundary conditions are applied to both x and y directions.

A crucial part of the Minimum Energy Path analysis is to prepare an energetically stable, dislocation-free reference state with and without the surface irregularity. We noticed that the dangling atomic bonds on the (001) surfaces cause major energy disturbances to the calculations due to random surface reconstructions. This is because that the free surface atoms, each having 3 dangling bonds, tend to randomly form clusters with neighboring atoms and release bonding energy, yielding either random or non-convergent result. To eliminate these disturbing factors, we form dimer bonds in the [110] direction by manually displacing surface atoms toward each other, as shown in Fig. 3(b). The system is then relaxed to a local energy minimum that has a much lower energy than the initial. We found that such a systematic surface reconstruction is indispensable during energy barrier calculations. Without such preparation, the numerical results are not repeatable. We use the reconstructed state as the starting point of energy barrier calculation and MD simulations.

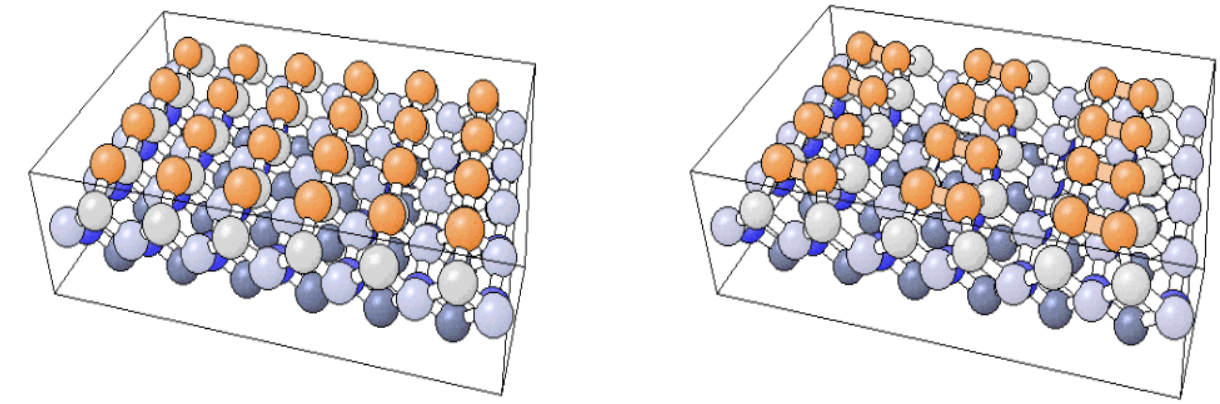

(a) before surface reconstruction

(b) dimer-constructed configuration

Figure 3: Displacing surface atoms to reconstruct dimers out of dangling bonds. Yellow atoms are on (001) surface.

3.4. Nested Sampling Method

Nested sampling (NS) is a Bayesian statistical method [**??**] adapted to explore the atomic phase space [**?**]. The NS algorithm does not require prior knowledge of the phases or phase transitions and takes only the potential energy function together with the desired pressure and temperature ranges as inputs. Moreover, the direct output of the simulation is the partition function as an explicit function of its natural variables, so calculating different thermodynamic observables, such as compressibility or heat capacity, is straightforward.

NS has been applied to study clusters and the hard-sphere model [**???**], and it has been shown that the NS algorithm enables the automated calculation of the complete pressure-temperature-composition phase diagram [**??**].

The nested sampling calculations of the current work were performed using the pymatnest program package [**?**] as presented in **?**. The simulations were run at constant pressure, and the simulation cell of variable shape and size contained 64 atoms. The initial configurations were generated randomly. New samples were generated with performing Hamiltonian Monte Carlo **?** (all-atom) moves, and changing the volume and the shape of the cell by shear and stretch moves, introducing swap moves in the bicomponent systems. Overall XXX steps were performed at every iteration with ratio 1:2:2:2, respectively. The number of walkers were chosen such that the difference in the melting temperature predicted by independent parallel runs is less than 100 K...XXX.

4. 0K energy barrier for dislocation nucleation

For semiconductor fabrications, dislocations usually nucleate from a free surface or phase boundary, homogeneous nucleation is practically unlikely. In this section, we perform energy barrier calculations with both the improved MEAM potential and SW. The geometry considered is a thin film of which the free surface is perturbed by a rectangular pit of a few atomic layers. Such a geometry is motivated by practical semiconductor devices, e.g., Grydlik et al. (2012), where a Si(001) template patterns with an array of pits of (111) side facets. Further more, having the pit structure is a way to mimic a roughened surface morphology that forms during SiGe thin film annealing. We refer to [cite zhang, cai] for detailed discussion.

Fig. 4 shows the NEB calculations with both MEAM and SW potential. It is observed that the results from both potentials are consistent. The NEB calculations show that the energy barrier for nucleating a dislocation in such a surface pit thin film will vanish after the compressive strain reaches 6% strain. In practice, the semiconductor system cannot sustain such a large strain energy. Some other failure mode will precede. See cite[zhang, cai]. However, it is not our intention here to identify or discover what nucleation mechanism should come at first place during the deposition process, which has been a puzzling problem for decades. The numerical calculation shows that the 0K energy barrier of the improved MEAM potential is "at least" as accurate as SW potential. And note that SW potential has been the dominant potential applied to study related problems.

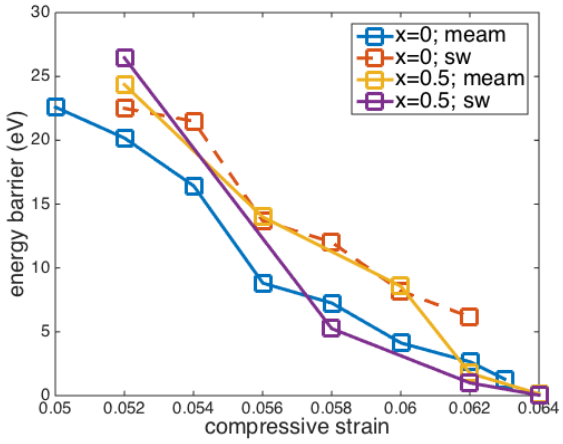

Figure 4: Lattice constants of $Si_{1-x}Ge_x$.

5. Melting Temperature calculation

Livia: can you put in related results/plots of melting temperature here. The calcualtions may include x =0, 0.25, 0.5, 0.75, 1. We can compare pure Si and pure Ge with previous works. Also, please clarify the "definition" of melting point in your calculation. Ideally, for each x, we should have both SW and meam.

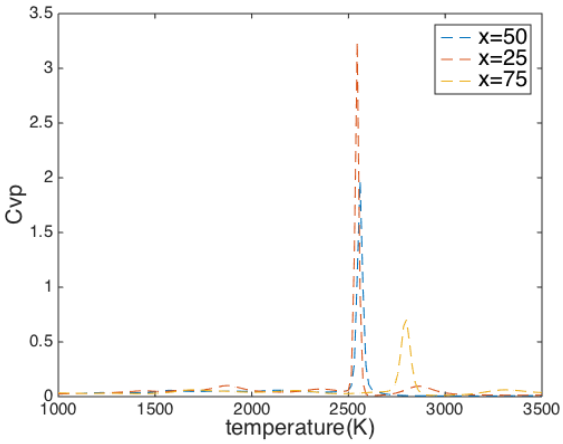

Figure 5: Lattice constants of $Si_{1-x}Ge_x$.

Can the four properties other than T_m be easily extracted from NS? If not, please modify the table accordingly.

Table 3: Thermal properties of Si, Ge, and SiGe as predicted by both SW and MEAM potentials and compared with experiments [1416]. The properties include the melting point Tm (K), latent heat of fusion L (Jg1), solid and liquid entropy at melting point, SS and SL (Jmol1 K1), and thermal expansion coefficient α ($106K1$) at 300K.

Element	Model	T_m	L	S_s	S_L	α
Si	MEAM	0				
Si	SW	0				
Si	Exp	1687				
Ge	MEAM	1216				
Ge	SW	2898				
Ge	Exp	1211				
$Si_{0.5}Ge_{0.5}$	MEAM	0				
$Si_{0.5}Ge_{0.5}$	SW	0				
$Si_{0.5}Ge_{0.5}$	Exp	1108				

5.1. Stress strain response at high temperature

5.1.1. Tech details to be commented

1. pure silicon, 0K, SW underestimates shear modulus: C44 is less than experiment by 30%., C12 is larger by 25 30%.

   e.g.,

   Molecular dynamic calculation of elastic constants of silicon, 1986 Comparative study of silicon empirical interatomic potentials, 1992

2. The experimental value for silicon shear modulus varies from 50.9 GPa to 79.4 GPa. According to NSM webpage it is 51GPa. http://www.ioffe.ru/SVA/NSM/Semicond/SiGe/mechanic.html

3. The 0K stress strain curves with the new potential. The shear modulus for pure Si is 56 GPa (meam) and 42 GPa (sw). The system I tested is [1-2 1] x [111] x[10-1]. shear along yz direction. For Ge, SW and MEAM are consistent. With increasing Ge concentration, the difference between SW and MEAM becomes smaller.

4. 0K stress strain curve of SW: mc2:/home/xzhang11/Planet/Libs/MD++.svn/runs/ho-sige-DN, scripts: mc2:/home/xzhang11/Planet/Libs/MD++.svn/scripts/work/SiGeHomo-sworig/ss_sige.tcl)
   0K stress strain curve of MEAM: mc2:/home/xzhang11/Planet/Libs/MD++.svn/runs/ho-sige-DN-meam, scripts: mc2:/home/xzhang11/Planet/Libs/MD++.svn/scripts/work/SiGeHomo-sworig/ss_sige.tcl)
   matlab>>plot(strain(:,2),stress(:,6))

One can conclude that the dislocation nucleation in bulk requires significantly larger energy, which implies that a dislocation is hardly possible to nucleate homogeneously. However, the shear stress strain relationship from a bulk system reveals the fundamental strength and load capacity, therefore, a good way to examine

the potential difference. The goal of this section is to demonstrate that the predictability of SW at high temperature is seriously undermined because of its failure in giving accurate thermal properties.

Fig. 6 shows the x-y shear stress and strain relationship at different temperatures. It is clearly observed that SW leads to earlier structural instabilities at elevated temperatures, compared to MEAM potential. At low temperature regime, the two potentials are satisfactorily consistent.

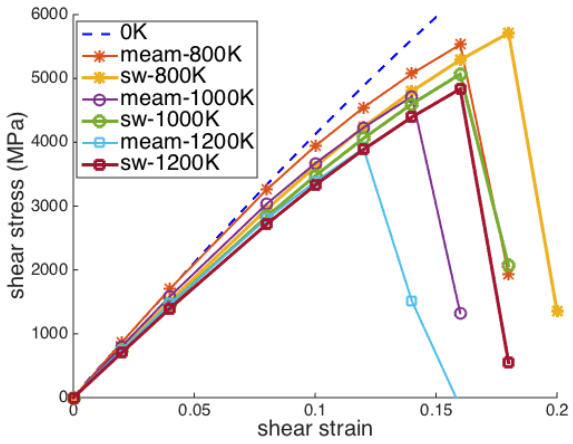

Figure 6: Lattice constants of $Si_{0.95}Ge_{0.05}$.

6. Conclusions and Future Works

We improved a Modified Embedded Atom Method potential for numerical studies of dislocation nucleation in Si_xGe_{1-x}. The potential is demonstrated to produce consistent mechanical properties as Stillinger-Weber potential. The melting temperature calculated from Nested Sampling method matches closely with experimental measurements. Energy barrier calculation shows that the nucleation barrier of the MEAM potential is consistent with hat predicted by SW. We point out the fact that SW is not appropriate to study high temperature SiGe plastic behaviors under high temperature semiconductor fabrications due to its unrealistic melting temperature. Some fundamental properties of the potential is calculated and compared to SW and Tersoff. It is found that Tersoff leads to much more stiff system than the other two potentials.

7. Acknowledgement

This work is supported by Samsung SSI (X.Z) and supported by the U.S. Department of Energy, Office of Basic Energy Sciences, Division of Materials Sciences and Engineering under Award No. DE-SC0010412 (W.C.).

References

J. Godet, P. Hirel, S. Brochard, L. Pizzagalli, Evidence of two plastic regimes controlled by dislocation nucleation in silicon nanostructures, 2009.

L. Pizzagalli, J. Godet, J. Guénolé, S. Brochard, E. Holmstrom, K. Nordlund, T. Albaret, A new parametrization of the stillinger–weber potential for an improved description of defects and plasticity of silicon, Journal of Physics: Condensed Matter 25 (2013) 055801.

S. Ryu, W. Cai, Comparison of thermal properties predicted by interatomic potential models, Modelling and Simulation in Materials Science and Engineering 16 (2008) 085005.

K. Kang, W. Cai, Brittle and ductile fracture of semiconductor nanowires–molecular dynamics simulations, Philosophical Magazine 87 (2007) 2169–2189.

K. Kang, W. Cai, Size and temperature effects on the fracture mechanisms of silicon nanowires: molecular dynamics simulations, International Journal of Plasticity 26 (2010) 1387–1401.

G. Grochola, S. P. Russo, I. K. Snook, A modified embedded atom method interatomic potential for alloy sige, Chemical Physics Letters 493 (2010) 57–60.

M. Baskes, Modified embedded-atom potentials for cubic materials and impurities, Physical Review B 46 (1992) 2727.

B.-J. Lee, J.-H. Shim, M. Baskes, Semiempirical atomic potentials for the fcc metals cu, ag, au, ni, pd, pt, al, and pb based on first and second nearest-neighbor modified embedded atom method, Physical Review B 68 (2003) 144112.

B.-J. Lee, M. Baskes, H. Kim, Y. K. Cho, Second nearest-neighbor modified embedded atom method potentials for bcc transition metals, Physical Review B 64 (2001) 184102.

Y.-M. Kim, B.-J. Lee, M. Baskes, Modified embedded-atom method interatomic potentials for ti and zr, Physical Review B 74 (2006) 014101.

J. G. Swadener, S. T. Picraux, Strain distributions and electronic property modifications in si/ge axial nanowire heterostructures, Journal of applied physics 105 (2009) 044310.

D. Read, V. Tewary, Multiscale model of near-spherical germanium quantum dots in silicon, Nanotechnology 18 (2007) 105402.

M. Baskes, Determination of modified embedded atom method parameters for nickel, Materials Chemistry and Physics 50 (1997) 152–158.

J. H. Rose, J. R. Smith, F. Guinea, J. Ferrante, Universal features of the equation of state of metals, Physical Review B 29 (1984) 2963.

S. Ryu, C. R. Weinberger, M. I. Baskes, W. Cai, Improved modified embedded-atom method potentials for gold and silicon, Modelling and Simulation in Materials Science and Engineering 17 (2009) 075008.

J. Dismukes, L. Ekstrom, E. Steigmeier, I. Kudman, D. Beers, Thermal and electrical properties of heavily doped ge-si alloys up to 1300 k, Journal of Applied Physics 35 (1964) 2899–2907.

Y. Wang, A. Santana, W. Cai, Au–ge meam potential fitted to the binary phase diagram, Modelling and Simulation in Materials Science and Engineering 25 (2016) 025004.

S. Plimpton, Fast parallel algorithms for short-range molecular dynamics, Journal of computational physics 117 (1995) 1–19.

M. Grydlik, F. Boioli, H. Groiss, R. Gatti, M. Brehm, F. Montalenti, B. Devincre, F. Schäffler, L. Miglio, Misfit dislocation gettering by substrate pit-patterning in sige films on si (001), Applied Physics Letters 101 (2012) 013119.